JVST A
Journal of Vacuum Science & Technology A

Imaging and direct manipulation of nanoscale three-dimensional features using the noncontact atomic force microscope

Cite as: Journal of Vacuum Science & Technology A **16**, 1425 (1998); https://doi.org/10.1116/1.581162
Submitted: 13 October 1997 . Accepted: 09 February 1998 . Published Online: 27 October 1998

T. R. Ramachandran, A. Madhukar, P. Chen, and B. E. Koel

View Online

Export Citation

ARTICLES YOU MAY BE INTERESTED IN

Nanoscale potential measurements in liquid by frequency modulation atomic force microscopy
Review of Scientific Instruments **81**, 123705 (2010); https://doi.org/10.1063/1.3514148

Calibration of atomic-force microscope tips
Review of Scientific Instruments **64**, 1868 (1993); https://doi.org/10.1063/1.1143970

HIDEN ANALYTICAL
Instruments for Advanced Science
▪ Knowledge,
▪ Experience,
▪ Expertise
Click to view our product catalogue
Contact Hiden Analytical for further details:
W www.HidenAnalytical.com
E info@hiden.co.uk
Gas Analysis
▸ dynamic measurement of reaction gas streams
▸ catalysis and thermal analysis
▸ molecular beam studies
▸ dissolved species probes
▸ fermentation, environmental and ecological studies
Surface Science
▸ UHV TPD
▸ SIMS
▸ end point detection in ion beam etch
▸ elemental imaging - surface mapping
Plasma Diagnostics
▸ plasma source characterization
▸ etch and deposition process reaction kinetic studies
▸ analysis of neutral and radical species
Vacuum Analysis
▸ partial pressure measurement and control of process gases
▸ reactive sputter process control
▸ vacuum diagnostics
▸ vacuum coating process monitoring

© 1998 American Vacuum Society.

Imaging and direct manipulation of nanoscale three-dimensional features using the noncontact atomic force microscope

T. R. Ramachandran,[a] A. Madhukar,[b] P. Chen, and B. E. Koel[c]
Department of Materials Science and Engineering and Laboratory for Molecular Robotics, University of Southern California, Los Angeles, California 90089

(Received 13 October 1997; accepted 9 February 1998)

We report on a remarkable image contrast reversal in noncontact atomic force microscope (NC-AFM) imaging of nanosized three-dimensional (3D) particles. We show that the image contrast of such 3D particles can switch from positive to negative as a function of NC-AFM imaging conditions and this occurs during, both, *in situ* ultrahigh vacuum imaging and imaging in air. Our results indicate that the contrast reversal can arise from a tip-sample interaction force-gradient-dependent instability of the NC-AFM feedback loop. Exploiting the above instability to induce selective tip-sample contact, we propose and demonstrate a protocol for the controlled nanomanipulation of 5 nm diameter gold particles, in *air* at *room temperature* using the NC-AFM. The contrast reversal phenomenon is proposed to be universal, suggesting its potential applicability to nanomanipulation in a variety of materials systems. © *1998 American Vacuum Society.*
[S0734-2101(98)54703-3]

I. INTRODUCTION

The practical applications of the noncontact atomic force microscope (NC-AFM)[1] have largely surpassed the few attempts to date to theoretically understand the scientific basis of this technique. While the atomic resolution NC-AFM images[2–6] of ''two-dimensional'' (2D) flat surfaces are not well understood,[3–9] the interpretation of NC-AFM images of nanoscale (or larger) three-dimensional (3D) features is even more complicated due to the effects of the macroscopic tip shape[10] on such images. *In situ* NC-AFM studies in ultrahigh vacuum (UHV) of nanoscale 3D features have revealed considerable dependency of NC-AFM image contrast of such features on the imaging conditions.[11] Recently, the utility of the NC-AFM has been extended by its application to the direct manipulation in air of 15 nm[12] and 30 nm[13] sized nanoparticles. Such NC-AFM based manipulation can potentially compete with both contact AFM (C-AFM) based approaches[14,15] and with the achievements of UHV scanning tunneling microscope (STM) based manipulation of $\sim 1-2$ nm sized molecules.[16,17]

In this article we report results from a systematic study of NC-AFM imaging of nanoscale 3D features, in UHV and in air. Remarkably, the NC-AFM image contrast of the nanofeatures is found to reverse from positive to (partial-to-complete) negative as the imaging conditions are changed. Our results, as well as a simple force-gradient model, indicate that the contrast reversal is likely to be universal and that it may arise due to a feedback instability that could potentially bring the tip into contact with the 3D nanofeature. In the second part of this article, we exploit the above contrast reversal phenomenon for selectively inducing tip-nanofeature contact and accordingly propose a new approach for nanomanipulation using the NC-AFM. We demonstrate the reliability of this approach via the controlled nanomanipulation of randomly distributed 5 nm sized Au particles into a chainlike pattern. This approach also allows the pushing of nanoparticles over nanoscale surface protrusions and for pushing nanoparticle pairs.

II. EXPERIMENT

UHV NC-AFM studies were performed on InAs 3D nanoscale islands on GaAs,[18,19] prepared by depositing 1.74 ML of InAs on GaAs(001) via molecular beam epitaxy and transferring such samples *in situ* into the UHV NC-AFM chamber.[18] The samples used for NCAFM studies in air were: (i) cleaved mica surfaces having nanoscale mica particles, and (ii) 5–30 nm diameter gold particles deposited from a colloidal solution onto a freshly cleaved mica surface that was previously functionalized with a layer of poly-L-lysine.[12] The cantilevers (CLs) used had a nominal stiffness constant, k_0, of ~ 2.5 N/m (UHV) and ~ 18 N/m (air), and a natural resonance frequency, ν_0 of ~ 58 kHz (UHV) and ν_0 in the range of 300–400 kHz (air).[20]

Our UHV NC-AFM works by the principle of ''frequency modulation'' detection.[2,3,5,11,21] Briefly, the NC-AFM feedback brings an oscillating CL with a mounted tip towards the sample until the resonance frequency of the CL shifts from its natural value, ν_0 (when the tip is far away from the surface) to a user defined new value, ν_{set}, due to the interaction between the tip and sample. The amplitude of oscillation of the CL, A, is simultaneously feedback controlled to be equal to a user-defined value A_{set}. Typically, $\Delta\nu = \nu_{set} - \nu_0$, is negative[2] and NC-AFM images are obtained by scanning the CL/tip over the sample while maintaining ν_{set} and A_{set} constant. According to the simplest model of NC-AFM, valid in the limit of small A, the NC-AFM image corresponds to a map of constant force gradient experienced by the tip due to

[a] Electronic mail: trr@lipari.usc.edu
[b] Also with the Department of Physics.
[c] Also with the Department of Chemistry.

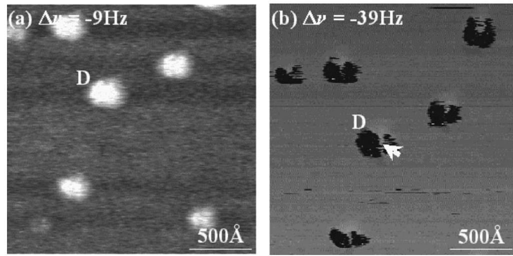

FIG. 1. UHV NC-AFM images of nanoscale 3D InAs islands in a 1.74 ML InAs/GaAs(001) sample, for fixed $A_{\rm set}$=66 nm. In (a), for $\Delta\nu=-9$ Hz the 3D islands (labeled D) appear in positive contrast. In (b), for $\Delta\nu=-39$ Hz, the same islands (D) appear in almost complete negative contrast. The arrow in (b) points to instabilities in the scan in the negative contrast region.

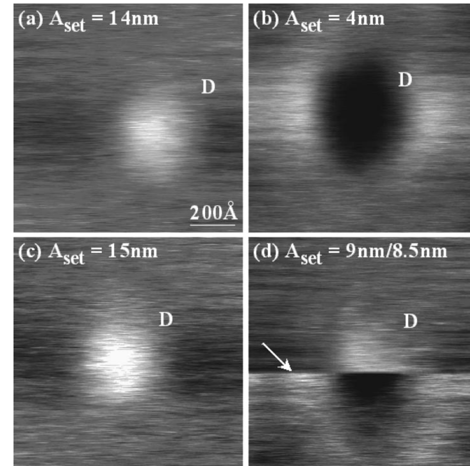

FIG. 2. NC-AFM images in air ($\nu_{\rm set}$~309.14 kHz) of the same 3D nanoparticle (marked D) on mica. This particle images in positive contrast for (a) $A_{\rm set}$=14 nm, in negative contrast for (b) $A_{\rm set}$=4 nm, and positive again for (c) $A_{\rm set}$=15 nm. In (d), the abruptness of the contrast change is seen. In the top part of (d) (positive contrast of nanoparticle) $A_{\rm set}$=9 nm, and at the point of the arrow $A_{\rm set}$ was reduced to 8.5 nm, causing negative contrast of the particle in the lower part.

its interaction with the sample.[1,22] For a CL of mass m, the effective resonance frequency, $\nu_{\rm eff}$, of the CL due to the presence of the sample can be given by:[1,22]

$$\nu_{\rm eff}=\frac{1}{2\pi}\sqrt{\frac{k_0-F'(z)}{m}} \quad (1)$$

where, $F'(z)$ is the force gradient experienced by the NC-AFM tip due to the sample, z is an *effective* tip-sample separation, and $\nu_{\rm eff}=\nu_{\rm set}$ during NC-AFM imaging. In principle, Eq. (1) also governs the working principle of our ambient NC-AFM, although this instrument works via ''amplitude modulation'' detection[23] where the change in A accompanying the shift in the CL resonance upon approaching the sample is exploited. The CL is initially *driven* slightly above its resonance ($\nu_{\rm set}>\nu_0$) when it is far away from the sample. Then, the user specifies a value $A_{\rm set}$ that is lower than $A(\nu_{\rm set})$ and the feedback moves the tip towards the sample until the CL oscillation amplitude at $\nu_{\rm set}$ decreases to the value $A_{\rm set}$. This would be expected to occur when the resonance response of the CL is shifted towards the lower end of the spectrum on approaching the sample.[21,23] The NC-AFM image is now acquired by maintaining, for the CL, the value $A_{\rm set}$ at the user-defined $\nu_{\rm set}$.[24] In general, during NC-AFM imaging the cantilever is brought closer on average to the sample by the feedback when $A_{\rm set}$ is decreased from its instantaneous value keeping $\nu_{\rm set}$ fixed (in both the UHV and ambient NC-AFMs above) or if $\nu_{\rm set}$ is lowered (making $\Delta\nu$ more negative) keeping $A_{\rm set}$ fixed (for the UHV NC-AFM).[2,4,11]

III. RESULTS AND DISCUSSION

A. NC-AFM imaging of nanoscale 3D features

Figure 1 shows *in situ* UHV NC-AFM images of 3D nanoscale InAs islands on GaAs(001) for fixed $A_{\rm set}$= 66 nm but with varying $\Delta\nu$. In (a), where $\Delta\nu=-9$ Hz, the islands appear in positive contrast as ~2–4 nm high protrusions (''bright dots''), as expected based on C-AFM images of such samples.[18,19] However, in (b), the same islands (labeled D) appear in almost complete negative contrast (dark spots) for $\Delta\nu=-39$ Hz. The arrow in (b) points to some instabilities that often occur within the negative contrast region. The image contrast also shows a change from positive to negative (defined always with respect to the surrounding flat area) when $A_{\rm set}$ is decreased with $\Delta\nu$ (i.e., $\nu_{\rm set}$) fixed, as previously reported.[11] The negative contrast is defined here to be either partial (as shown below) or complete (when it covers the whole 3D feature).

Figure 2 shows NC-AFM images taken in air of a 3D mica nanofeature on mica, with $\nu_{\rm set}$~309.14 kHz (ν_0 ~309.00 kHz). In Fig. 2(a) the feature (labeled D) appears in positive contrast (~1 nm high) for $A_{\rm set}$=14 nm, but it appears in complete negative contrast for $A_{\rm set}$=4 nm [panel (b)] where the CL is, on average, closer to the surface. When $A_{\rm set}$ is reset to 15 nm [panel (c)], the feature is once again imaged in positive contrast, exhibiting a reversibility in the contrast reversal. The abruptness of the contrast reversal is illustrated in panel (d) for the same nanofeature. Here, the top part of the image was acquired with $A_{\rm set}$=9 nm and at the line marked by the arrow $A_{\rm set}$ was decreased to 8.5 nm, which immediately changes the image contrast from positive to negative. We find that *every* sample containing nanoscale 3D features which we examined in UHV and in air exhibited this unusual contrast reversal phenomenon, but to varying degrees. For instance, Fig. 3 shows an example where the negative contrast is only partial. Figure 3(a) is a positive contrast NC-AFM image in air of 5 nm diameter gold particles[25] on poly-L-lysine covered mica for $A_{\rm set}$=5 nm. On the other hand, Fig. 3(b) ($A_{\rm set}$=4 nm, same $\nu_{\rm set}$) shows that the same particles (two of which are labeled 1 and 2) have a central region of partial negative contrast (dark spot labeled by an arrow).

The fact that contrast reversal in NC-AFM images of nanoscale 3D features is observed, as a function of varying $A_{\rm set}$ or $\nu_{\rm set}$ (i.e., $\Delta\nu$), in contamination-free, *in situ* UHV NC-AFM images as well as in air indicates that this might be

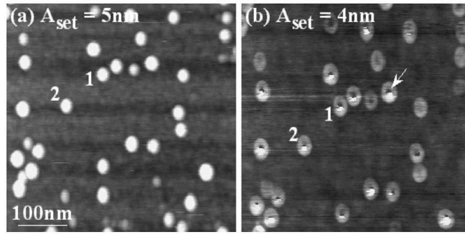

FIG. 3. NC-AFM images in air (ν_{set}~334.14 kHz) of 5 nm Au nanoparticles on poly-L-lysine covered mica. The nanoparticles appear in positive contrast in (a), for A_{set}=5 nm. In (b), for A_{set}=4 nm, the same nanoparticles (e.g., 1 and 2) exhibit partial negative contrast (arrow).

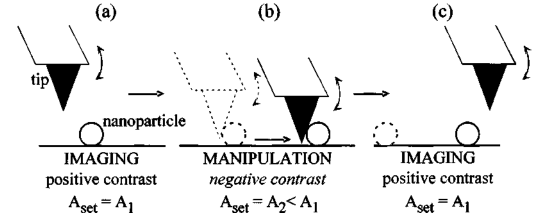

FIG. 5. Schematic of our NC-AFM based manipulation protocol, as applied to our ambient AFM. In (a), the tip is in the positive contrast imaging mode ($A_{set}=A_1$, region III of Fig. 4), positioned a few nm above the nanoparticle and approaching it. In (b), A_{set} is decreased to $A_2<A_1$ to make the tip enter the negative contrast regime *and* to then induce tip-sample contact. With A_{set} fixed at A_2 and the tip moving in the desired direction [see (b)] the particle is also moved. Then, A_{set} is reset to A_1 and the NC-AFM is brought back into the imaging mode (c).

a universal phenomenon observable in any environment. Clearly, the complexity of the NC-AFM imaging process for finite values of A_{set}[2,5,9] preclude a straightforward explanation of this phenomenon using Eq. (1). However, it is useful to examine the consequences of the simplified model of Eq. (1) to find out if, and how, contrast reversals can arise in NC-AFM even within this force-gradient model.

Figure 4 shows schematic curves depicting the force $F(z)$ and force-gradient $F'(z)$ experienced by the tip due to the sample as a function of z. Here, z_A corresponds to the value of z at the minimum detectable force gradient, and thus $\Delta\nu$, in the NC-AFM, and $z_{A'}$ corresponds to the maximum force gradient. In region III ($z_{A'} \leqslant z \leqslant z_A$), as z decreases, $F'(z)$ increases and therefore, in Eq. (1), ν_{eff} decreases. The decrease in ν_{eff} with decreasing z is consistent with the design rule of our NC-AFM feedback that, as ν_{set} is decreased, the CL will be moved, on average, closer to the sample. Therefore, within the model described by Eq. (1), region III is the normal region of operation of our NC-AFMs (labeled ''stable feedback'') and in this region 3D protuberances on the surface will clearly be imaged in positive contrast. However, if z were to drop below $z_{A'}$ due to, say, attractive tip-sample interactions driving the tip towards the surface faster than the feedback response time (~1 ms), then the tip may enter region I (contact) or II. In these regions, as z decreases, $F'(z)$ decreases and ν_{eff} *increases*, which contradicts the working assumption of our NC-AFM feedback. Therefore, in this regime, a decrease in z will increase ν_{eff} and cause the feedback to move the CL even closer to the sample, in an attempt to ''decrease'' ν_{eff} to ν_{set}, which is, of course, impossible. This leads to an unstable or ''runaway'' [11] feedback that will result in artifactual NC-AFM images showing partial-to-complete negative contrast of 3D protuberances. Accordingly, there would be a divergence in the error signal of ν_{set} (or A_{set} in the ambient NC-AFM) which may manifest as instabilities in the image within the negative contrast regions [e.g., see Fig. 1(b)]. It must be noted that in this case, the quoted value of ν_{set} (or A_{set}) is only a nominal one and not necessarily the actual value, inside the negative contrast region. Furthermore, the negative contrast can potentially lead to tip-sample contact (region I), as we indeed observe in the form of surface destruction under prolonged scanning at pronounced negative contrast (not shown; also see Ref. 26). Thus, a feedback instability linked to the nature of the force gradient curve can account for image contrast reversal of 3D nanofeatures even within the simplified force-gradient model of NC-AFM imaging [Eq. (1)].

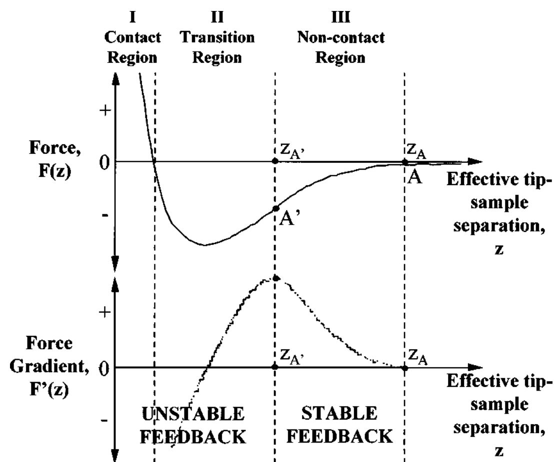

FIG. 4. Schematic of the force $F(z)$ and force gradient $F'(z)$ on the tip due to the sample, as a function of the effective tip-sample separation, z. Region I is the usual C-AFM regime. We label I/II and III as regions of unstable and stable NC-AFM feedback, respectively, based on the outcome of the force-gradient model of NC-AFM imaging and the feedback mechanism.

B. NC-AFM based direct manipulation of nanoscale 3D features

The contrast reversal phenomenon, while being an artifact, has at the same time the advantage of specifying *qualitatively* the regime of tip-sample interaction. The latter fact can be exploited as shown below to induce selective tip-sample contact with the view of directly manipulating nanoscale 3D features such as clusters or large molecules. Figure 5 schematically depicts a protocol we propose for such nanomanipulation using the example of the ambient NC-AFM. The procedure involves initially obtaining a NC-AFM image of nanoparticles on a surface with a value of $A_{set}=A_1$ which produces positive contrast of the particles. Next, we choose a particle of interest and perform a single line scan over the center of the particle in a desired direction with $A_{set}=A_1$.

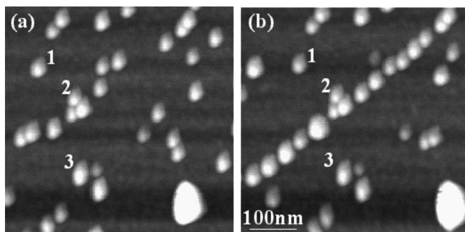

FIG. 6. NC-AFM images of 5 nm Au nanoparticles in air, (a) before and (b) after directed manipulation using the procedure in Fig. 5, with $A_1 = 5$ nm, $A_2 = 1$ nm. The random group of Au nanoparticles in (a) was rearranged to create the ''chain'' structure in (b) (labels 1–3 denote the same particles in both images). The feature in the lower right corner is a 15 nm high Au particle.

Then, a second line scan is commenced [Fig. 5(a)] but as the tip nears the particle A_{set} is decreased by computer control to a new value $A_2 < A_1$. The value A_2 is chosen so that we would not only operate in the negative contrast regime with respect to the nanofeature but *also* such that tip-nanofeature contact [region I of Fig. 4(b)] would occur [Fig. 5(b)]. The value of A_{set} is maintained at A_2 for a chosen interval of time (or equivalently, distance) and this has the effect of moving the nanoparticle along the sample surface in the direction of the scanning tip. Once the particle is moved over a desired distance, the computer resets A_{set} back to A_1 and goes back into the normal imaging mode [Fig. 5(c)]. The manipulation protocol depicted in Fig. 5 has been automated and the details of the computer control software are discussed elsewhere.[12]

Evidence for the viability of the above protocol is shown in Figs. 6–8, all acquired in air with $A_{set} = 5$ nm and $\nu_{set} \sim 394.86$ kHz ($\nu_0 \sim 394.51$ kHz). All nanomanipulation was performed in air, at room temperature, with $A_1 = 5$ nm and $A_2 = 1$ nm corresponding to the discussion above. Figure 6 shows NC-AFM images of a sample containing mostly 5 nm diameter Au particles,[25] (a) before and (b) after nanomanipulation using the above protocol. A spatially random collection of 5 nm Au particles in Fig. 6(a) (with a lone 15 nm particle seen as the brightest feature in the lower right corner) was rearranged in a predetermined manner to form the chainlike arrangement of Fig. 6(b). The labels 1–3 in panels (a) and (b) show, as a reference, the same three particles that were left untouched.

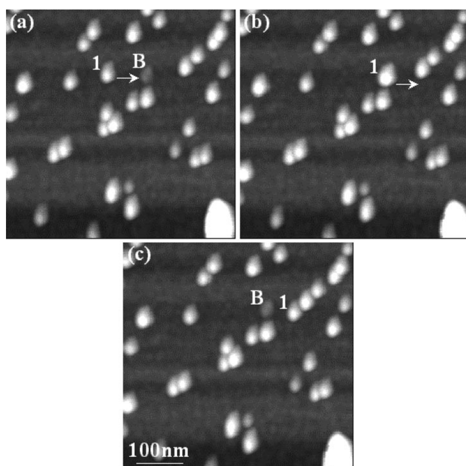

FIG. 7. NC-AFM images in air showing that nanoparticles can be moved over surface protrusions using the protocol of Fig. 5 (with $A_1 = 5$ nm, $A_2 = 1$ nm). The particle 1 in (a) was moved (arrow) towards an ~ 2 nm high protrusion, B. In (b) the particle 1 is observed to sit on top of B. Particle 1 was then moved again (c, arrow) to a new location making B visible again.

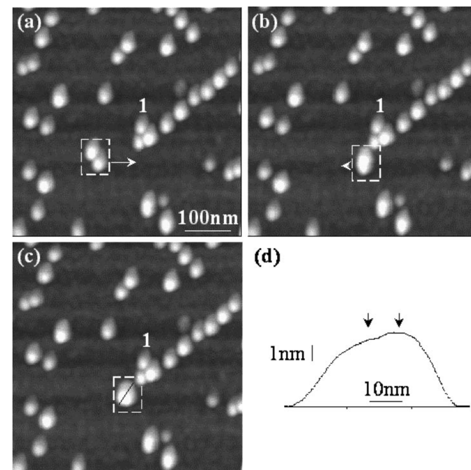

FIG. 8. NC-AFM images in air showing how a nanoparticle pair can be moved using the protocol of Fig. 5 ($A_1 = 5$ nm, $A_2 = 1$ nm). Panel (a) shows a pair of 5 nm Au nanoparticles (box). The tip was run roughly through the middle of this pair from left to right (arrow) resulting in (b) where the pair is seen to have moved and combined to form a larger (lateral size) feature. This larger feature was then moved (arrow, b) to produce the result in (c). The label 1 identifies a nanoparticle common to all images. Panel (d) shows a cross section across the pair of particles enclosed in the box in (c). The arrows in (d) mark the positions of the two particles in the pair.

Figure 7 shows how our protocol is successful in moving nanoparticles up and over nanoscale surface protrusions. The particle labeled 1 in Fig. 7(a) was moved in the direction of the arrow towards a ~ 2 nm high surface protrusion labeled B. The particle 1 was first brought to rest on top of B and then imaged in Fig. 7(b), seen as a brighter feature and labeled 1. Then, the particle was moved away from B in the direction of the arrow in Fig. 7(b) to its new position in Fig. 7(c) where, once again, both features 1 and B are revealed. Figure 8 shows how a nanoparticle pair was manipulated using the above protocol. Here, the tip was forced to follow a path that approximately bisected the two particles in Fig. 8(a) (rectangular box) in the direction of the arrow. The result is seen in panel (b) showing a new feature (box) that appears larger (in lateral size) than either of the particles in the pair [box in panel (a)]. The combined pair was then moved slightly in the direction of the arrow in panel (b) to a new position in panel (c). For reference, the same feature labeled 1 is shown in panels (a) through (c). Panel (d) shows a cross-sectional profile over the nanoparticle pair in the box in panel (c), corresponding to the black line shown within this box. The arrows in (d) mark the positions of the two particles in the pair.

Finally, we discuss some of the limitations and advantages of the above method. The main limitation of this technique is that tip-sample contact sometimes results in drastic

changes to the tip, which affects the quality of subsequent NC-AFM images and sometimes the reproducibility of manipulation. There is also the possibility of physical damage to the sample. The advantages of this technique are that: (a) it can be potentially used in any environment, (b) it can be used for a variety of materials systems, and (c) it relies only on the negative contrast phenomenon, which allows qualitative identification of the manipulation regime independent of the user or the material system. Our results suggest that the manipulation approach discussed here would be most successful when applied to materials systems where the nanoparticles are bound to the substrate via relatively weak electrostatic and/or van der Waals bonds. Particles bound via strong covalent bonds are usually immovable even during C-AFM operation.

IV. CONCLUSION

In conclusion, we have presented a remarkable contrast reversal phenomenon in NC-AFM imaging of nanoscale 3D features. Experimental evidence and the analysis of a force-gradient model of NC-AFM imaging indicate that this phenomenon could be attributed to a feedback instability associated with the nature of the tip-sample interaction force gradient curve. Exploiting the potential tip-sample contact ensuing from the negative contrast, we have proposed and demonstrated the viability of a new protocol for NC-AFM based nanomanipulation via a controlled rearrangement of 5 nm Au particles to form a chainlike pattern. We emphasize the universality of the contrast reversal phenomenon and its applicability to nanomanipulation in a variety of materials systems, potentially even to molecules (e.g., C_{60}) on surfaces.

ACKNOWLEDGMENTS

The authors thank Dr. C. Baur and Dr. A. Bugacov for help in the preparation of the Au/mica samples and C. Gazen and Professor A. Requicha for help on the NC-AFM control software. This work was carried out under support from the Zohrab A. Kaprielian Technology Innovation Fund of USC.

[1]R. Wiesendanger, *Scanning Probe Microscopy and Spectroscopy* (Cambridge University Press, Great Britain, 1994).
[2]F. J. Giessibl, Science **267**, 68 (1995).
[3]Y. Sugawara, H. Ueyama, T. Uchihashi, M. Ohta, S. Morita, M. Suzuki, and S. Mishima, Appl. Surf. Sci. **113/114**, 364 (1997).
[4]P. Guthner, J. Vac. Sci. Technol. B **14**, 2428 (1996).
[5]R. Luthi, E. Meyer, M. Bammerlin, A. Baratoff, T. Lehmann, L. Howald, Ch. Gerber, and H. J. Güntherodt, Z. Phys. B **100**, 165 (1996).
[6]R. Erlandsson, L. Olsson, and P. Martensson, Phys. Rev. B **54**, R8309 (1996).
[7]R. Perez, M. C. Payne, I. Stich, and K. Terakura, Phys. Rev. Lett. **78**, 678 (1997).
[8]U. Hartmann, Phys. Rev. B **43**, 2404 (1991).
[9]B. Anczykowski, D. Kruger, and H. Fuchs, Phys. Rev. B **53**, 15485 (1996).
[10]J. E. Griffith and D. A. Grigg, J. Appl. Phys. **74**, R83 (1993).
[11]T. R. Ramachandran, N. P. Kobayashi, R. Heitz, P. Chen, and A. Madhukar, Mater. Res. Soc. Symp. Proc. **440**, 31 (1997).
[12]C. Baur, B. C. Gazen, B. E. Koel, T. R. Ramachandran, A. A. G. Requicha, and L. Zini, J. Vac. Sci. Technol. B **15**, 1577 (1997).
[13]T. Junno, K. Deppert, L. Montelius, and L. Samuelson, Appl. Phys. Lett. **66**, 3627 (1995).
[14]Y. Kim and C. M. Lieber, Science **257**, 375 (1992); R. Luthi, E. Meyer, H. Haefke, L. Howald, W. Gutmannsbauer, and H. J. Güntherodt, *ibid.*, **266**, 1979 (1994); D. M. Schaefer, R. Reifenberger, A. Patil, and R. P. Andres, Appl. Phys. Lett. **66**, 1012 (1995).
[15]M. R. Falvo, S. Washburn, R. Superfine, M. Finch, F. P. Brooks, Jr., V. Chi, and R. M. Taylor, II, Biophys. J. **72**, 1396 (1997).
[16]M. T. Cuberes, R. R. Schlittler, and J. K. Gimzewski, Appl. Phys. Lett. **69**, 3016 (1996); T. A. Jung, R. R. Schlittler, J. K. Gimzewski, H. Tang, and C. Joachim, Science **271**, 181 (1996).
[17]P. H. Beton, A. W. Dunn, and P. Moriarty, Appl. Phys. Lett. **67**, 1075 (1995); S. Maruno, K. Inanaga, and T. Isu, *ibid.*, **63**, 1339 (1993).
[18]N. P. Kobayashi, T. R. Ramachandran, P. Chen, and A. Madhukar, Appl. Phys. Lett. **68**, 3299 (1996).
[19]J. M. Moison, F. Houzay, F. Barthe, L. Leprince, E. Andre, and O. Vatel, Appl. Phys. Lett. **64**, 196 (1994).
[20]These CLs are commercially available from Park Scientific Instruments.
[21]T. R. Albrecht, P. Grutter, D. Horne, and D. Rugar, J. Appl. Phys. **69**, 668 (1991).
[22]B. Gady, D. Schleef, R. Reifenberger, D. Rimai, and L. P. DeMejo, Phys. Rev. B **53**, 8065 (1996).
[23]Y. Martin, C. C. Williams, and H. K. Wikramasinghe, J. Appl. Phys. **61**, 4723 (1987).
[24]For the *ambient* NC-AFM images reported here, ν_{set} was chosen to be typically $\sim$0.15–0.60 kHz higher than ν_0.
[25]The apparent lateral sizes of the 3D nanofeatures in the images shown in this article are larger than their actual sizes due to tip-size induced broadening.
[26]U. Durig and O. Zuger, Phys. Rev. B **50**, 5008 (1994). These authors reported the observation of negative contrast in UHV NC-AFM images of polycrystalline Ir. They found a ''cleansing effect'' on the surface, i.e., disappearance of certain features observed in positive contrast, due to repetitive scanning of the same area in which some features were imaged in negative contrast.